Chemical Identification of Ions in Doped NaCl by Scanning Force Microscopy

Adam S. Foster,[1,2] Clemens Barth,[3] and Claude R. Henry[3]

[1]*Helsinki University of Technology, Laboratory of Physics, P.O. Box 1100, 02015 Helsinki, Finland*
[2]*Department of Physics, Tampere University of Technology, P.O. Box 692, 33101 Tampere, Finland*
[3]*CINaM-CNRS, Campus de Luminy, Case 913, 13288 Marseille Cedex 09, France*

A quantitative comparison between experiment and theory is presented, which shows that all ions of the Suzuki structure on (001) surfaces of Mg^{2+} or Cd^{2+} doped NaCl crystals can be identified despite the tip-surface distance, differences in impurity chemistry, and surface termination. The identification can be used to calibrate the potential of the tip's last atom, and it is proposed to use these surfaces for better characterization of deposited nano-objects.

PACS numbers: 68.37.Ps, 68.35.Dv

Alkali halides have remained of intense scientific interest, due to their role in, for example, studies of molecular electronics [1–5] and cluster science [6–8], where they serve as insulating substrates. For the characterization of these surfaces, the dynamic scanning force microscope (SFM) [9] is increasingly becoming the tool of choice due to its universal applicability. A key ambition in studies is to obtain atomic resolution on both the substrate and adsorbed nano-object, providing a complete characterization of the system. Since the substrate geometry is generally known, interpretation of image contrast of the substrate should greatly aid in understanding the nano-object configuration. For ionic surfaces, atomic resolution imaging is mainly determined by the sign of the electrostatic potential from the tip apex [10], and for specific systems the contrast pattern observed directly identifies the character of the tip and ions on the surface. However, for the symmetric (001) surfaces of cubic crystals, images with tips of opposite potential are almost identical and cannot be distinguished [11,12]. In most cases, force spectroscopy at different atomic sites on the surface is needed for the identification of the surface ions [13,14], which demands a time-consuming comparison between experiment and theory—direct interpretation from conventional experimental images would certainly be strongly preferred.

It is well known that doping NaCl crystals with divalent impurity cations results in the precipitation of the so-called Suzuki phase [15,16]. Recent dynamic SFM studies of NaCl:Mg^{2+} confirmed that Suzuki precipitates are embedded in the NaCl matrix on the (001) surface [17]. Two different types of surfaces regions can be found, which are well separated [17,18] [Fig. 1(a)]. The atomic unit cell of the Suzuki phase is twice as large as the one of NaCl(001) and is composed of three different ions including Na$^+$ vacancies [Fig. 1(b)]. Because of the special geometry of the Suzuki structure, each type of ion can be resolved on the surface by dynamic SFM [17]. In this Letter, we show by comparison between experiment and theory that chemical identification can be provided independently of the tip-surface distance and chemistry of the

tip. By further comparison to the Suzuki phase of the NaCl:Cd^{2+}(001) surface, we show that this identification is consistent for impurities with dissimilar chemistry and different surface terminations.

Czochralski-grown NaCl crystals were doped with 1 mol % $MgCl_2$ or 2 mol % $CdCl_2$ [18]. The surfaces were prepared in UHV by cleavage at room temperature and annealing at 220 °C. Experiments were performed at 3×10^{-10} mbar, at room temperature with a dynamic SFM with a conductive silicon cantilever (p-Si, 0.015 Ω cm, 315 kHz resonance frequency, 37 N/m spring constant, 15 nm peak-to-peak amplitude). All images were acquired in the constant height mode and represent the detuning Δf of the cantilever resonance frequency. Dark contrast belongs to more negative detuning values (larger tip-surface attraction) [17].

Calculation of the tip-surface interaction and simulated images were performed via the general approach outlined in previous works [10], combining two-dimensional periodic atomistic simulations [19] and macroscopic van der Waals to provide the total force field across the surface. In simulated images, experimental values for cantilever parameters were used, and the tip radii (NaCl:Mg^{2+} ~20 nm and NaCl:Cd^{2+} ~100 nm) were determined via
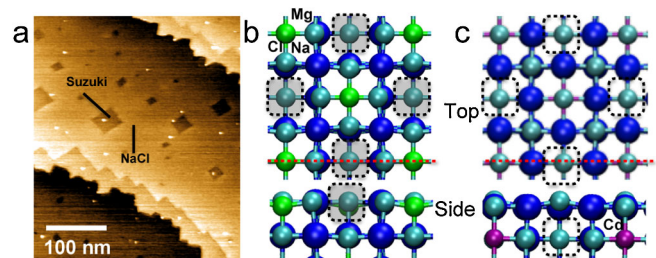

FIG. 1 (color online). (a) Topography image of Suzuki precipitates on the NaCl:Cd^{2+}(001) surface. Atomic structure of the (b) Suzuki terminated NaCl:Mg^{2+} surface and (c) NaCl-terminated NaCl:Cd^{2+} surface. The shaded and unshaded boxes indicate surface and subsurface vacancy sites, respectively. The dashed line shows the plane of the side view.

fitting to measured detuning vs distance curves. In combination with the agreement between simulated and experimental contrast magnitudes at different distances, this means we are matching both the experimental long-range and short-range forces in simulations. In atomistic simulations, the surface consists of a $2 \times 2 \times 1$ slab in terms of the 60 atom Suzuki unit cell. Since the original silicon tip is usually oxidized by exposure to air or contaminated by contact with the surface, the most likely tip terminations are one of the surface species or oxygen. Hence, for models of the tip apex we use seven different 64-atomic-site cubic nanoclusters: NaCl, NaCl terminated by Mg^{2+} or Cd^{2+}, $NaCl:Mg^{2+}$, $NaCl:Cd^{2+}$, and MgO. Each was oriented so that they are symmetric along the z axis, presenting one of 12 different electrostatic potentials to the surface. The bottom layer of the surface and top three layers of the tip are frozen during simulations, and all other atoms are allowed to relax. The potentials for MgO and $NaCl:Mg^{2+}$ are taken from Refs. [19,20].

In order to fit the remaining potentials and to check the accuracy of the atomistic simulations in general, calculations of the structures have also been performed using the spin-polarized density functional theory, projected augmented wave potentials (including semicore states for Na, Mg, and Cd), and the Perdew-Burke-Ernzerhof functional [21]. A kinetic energy cutoff of 300 eV (350 eV for $NaCl:Cd^{2+}$) and a k-point sampling of $3 \times 3 \times 3$ ($3 \times 3 \times 1$ for slab calculations) were found to converge the total energy of our systems to within meV. Surface relaxations were well converged for a slab four layers deep with a vacuum of 1.2 nm. Our calculated structures agreed well with previous experimental and theoretical studies [22,23]. The agreement between *ab initio* and atomistic results for the Suzuki bulk and surface equilibrium structures was excellent in all cases. However, since the contrast in SFM imaging has been previously shown to strongly de-

pend on tip-induced displacements [10], we also calculated the energy vs displacement curve for atoms of each sublattice of every surface in both approaches. The potential parameters were then tuned to reproduce the *ab initio* displacement curves, while maintaining agreement in basic structures.

In Fig. 2(a), three experimental images acquired inside a Suzuki precipitate are shown, along with corresponding profiles along the $\langle 100 \rangle$ and $\langle 110 \rangle$ surface direction [Figs. 2(b) and 2(c)]. The contrast pattern changes from an array of dark spots to a second, in-between, additional array of dark spots. At closest distance, the second type of dark spots is most pronounced. The size of the array formed by the latter dark spots equals the size of the sublattice formed by either the Mg^{2+} ions or Na^+ vacancies. Around each of the latter dark spots, four bright spots can be seen which match the sublattice formed by the Cl^- ions.

Simulations were best able to reproduce this contrast pattern and its dependence on tip-surface distance by using a Cl-terminated NaCl tip [24]. The overall quantitative agreement confirms the surface structure shown in Fig. 1(a). The main component in the distance dependence of the images is the increasing attraction between the tip and the Mg^{2+} sites in the surface. At long range, greater than 0.4 nm, the large displacement of Na^+ ion towards the tip [Fig. 3(a)] means that it dominates the interaction, despite having only half the charge of the Mg^{2+} ion, and determines the contrast in images at large distances [Fig. 2(c), top]. The more strongly bound Mg^{2+} is already 0.03 nm further into the surface in the absence of the tip and shows little displacement as the tip approaches [see Fig. 3(b)]. At closer approach, less than 0.4 nm, the surface Na^+ enters the repulsive interaction with the Cl^- tip, and the overall interaction over the Mg^{2+} becomes comparable [Fig. 2(c), middle]. At these tip-surface separations, the
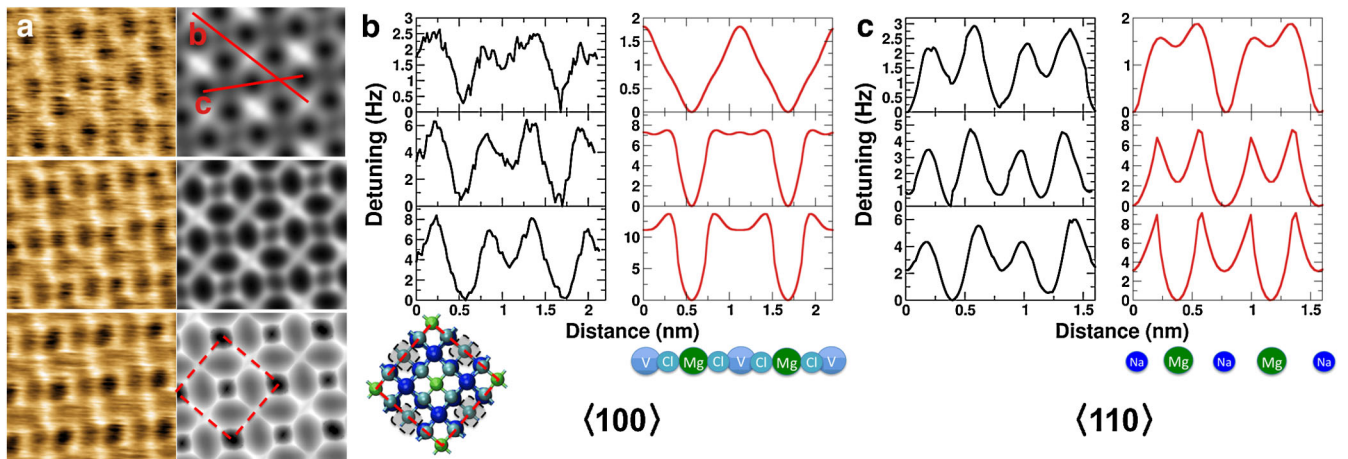

FIG. 2 (color online).   Comparison of experimental and simulated data for $NaCl:Mg^{2+}$. The simulations used a Cl-terminated NaCl tip. (a) Images (color: experiment, gray scale: theory), (b) scan lines (red is simulated) in the $\langle 100 \rangle$ direction, and (c) scan lines in the $\langle 110 \rangle$ direction. The experimental data correspond to an average detuning of -16, -22, and -24 Hz (top-bottom, with a more negative detuning corresponding to imaging closer to the surface). The simulated data correspond to tip-surface heights of 0.45, 0.325, and 0.275 nm, resulting in average detunings of -16.4, -21.8, and -23.0 Hz, respectively.
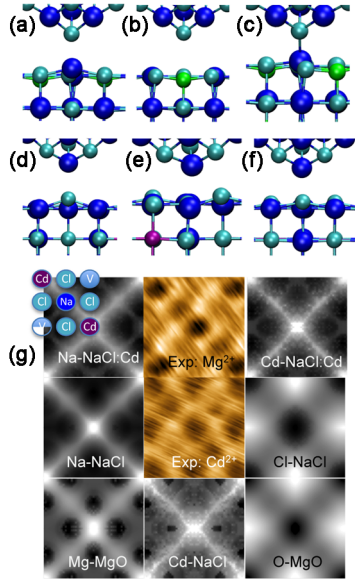
FIG. 3 (color online). Simulation snapshots showing key atomic displacements for a Cl-terminated NaCl tip imaging NaCl:Mg^{2+} at a tip height of (a) 0.4 nm over an Na$^+$ site, (b) 0.4 nm over an Mg site, (c) 0.26 nm over a Cl$^-$ site, and for a Na-terminated NaCl tip imaging NaCl:Cd^{2+} at a tip height of (d) 0.46 nm over a Cl$^-$ site above a vacancy, (e) 0.31 nm over an Na$^+$ site, and (f) 0.4 nm over a Cl$^-$ site above a Na$^+$. (g) Comparison of experimental images of NaCl:Mg^{2+} and NaCl:Cd^{2+} with simulated images of NaCl:Cd^{2+} using seven different tips X:Y (gray scale), where Y is the tip material and X is the terminating atom.

originally repulsive interaction between tip and surface Cl$^-$ is compensated by lateral displacements of neighboring Na$^+$ towards the tip [see Fig. 3(c)] resulting in the development of the double peak structure seen in scan lines [Fig. 2(b), middle]. At close distances (<0.3 nm), the interaction with the Mg^{2+} ions dominates [Fig. 2(c), bot-

tom]. In comparison to pure NaCl(001), the development of contrast as a function of tip-surface separation reflects a much richer variety of atomic processes. The presence of the vacancy sublattice plays an especially important role in increasing the possibility and magnitude of atomic displacements. Note that the limit of approach to the surface was the onset of instabilities due to atomic jumps, and contrast inversion was never observed.

Figure 4 shows the contrast development of experimental images and scan lines of the NaCl:Cd^{2+} Suzuki surface as the detuning is increased and the tip approaches the surface. At largest distance, the contrast is formed by large dark spots, which form a sublattice equal to the one formed by either the Cd^{2+} ions or the Na$^+$ vacancies and do not change with decreasing distance. At closest distance, four additional bright spots appear around each dark spot forming a sublattice of either Cl$^-$ or Na$^+$ ions. Additional dark spots appear more pronounced in between the large dark spots.

Initially, we considered that the NaCl:Cd^{2+} Suzuki surface termination includes both Cd^{2+} ions and Na$^+$ vacancies, as in the case of NaCl:Mg^{2+}. However, simulations were unable to reproduce the observed contrast with any tip, including tips based on the Suzuki structure itself [Fig. 3(g) and also see Ref. [24]]. Note also that the contrast differs considerably from that obtained on NaCl:Mg^{2+}(001). In order to understand this, we analyzed in detail the possible surface terminations of both NaCl:Mg^{2+} and NaCl:Cd^{2+} by varying the vacancy and impurity location in surface and subsurface layers while maintaining the size of the Suzuki unit cell. For NaCl:Mg^{2+}, we find that the lowest surface energy is for the Suzuki termination (0.18 J/m^2; NaCl termination is 0.22 J/m^2), as shown in Fig. 1(a). However, for NaCl:Cd^{2+} the surface energy for the Suzuki termination
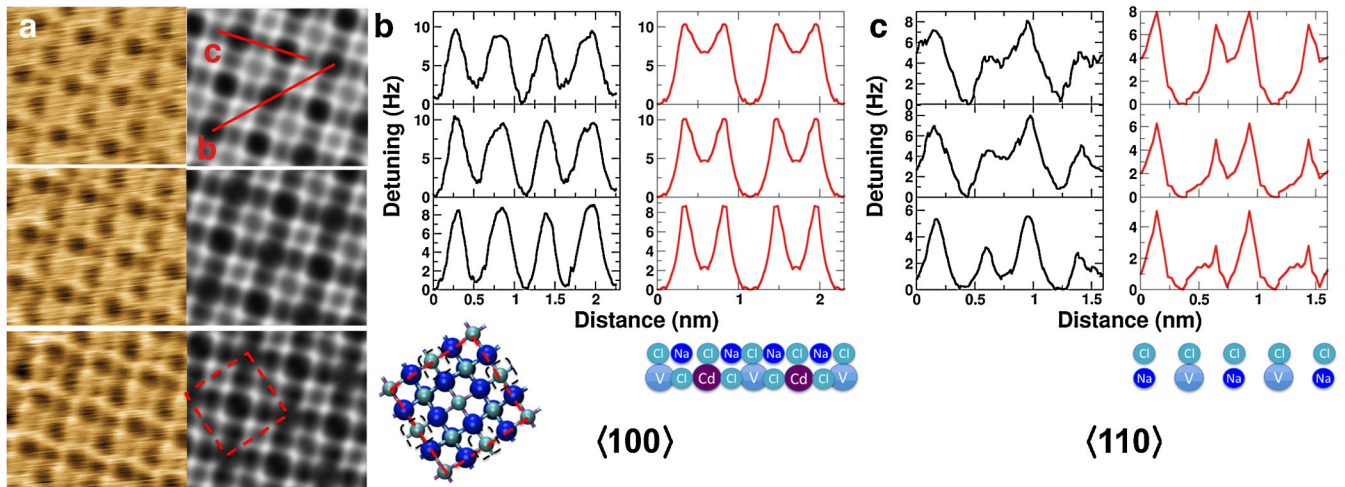

FIG. 4 (color online). Comparison of experimental and simulated data for NaCl:Cd^{2+}. The simulations used a Na-terminated NaCl tip. (a) Images (color: experiment, gray scale: theory), (b) scan lines (red is simulated) in the $\langle 100 \rangle$ direction, and (c) scan lines in the $\langle 110 \rangle$ direction. The experimental data correspond to an average detuning of -109, -112, and -115 Hz (top-bottom). The simulated data correspond to tip-surface heights of 0.375, 0.35, and 0.325 nm, resulting in average detunings of -107, -112, and -116 Hz, respectively.

(0.29 J/m^2) is higher than the minimum energy configuration with the uppermost layer consisting of a pure NaCl monolayer and the vacancies/impurities in the subsurface layer (0.21 J/m^2). This surface termination is shown in Fig. 1(b). Using the latter surface in SFM simulations, we were able to best reproduce the experimental images and scan lines with a Na-terminated NaCl tip, demonstrating that, in this case, the NaCl:Cd^{2+} Suzuki region most likely has a NaCl termination.

The development of contrast as the tip approaches the surface (see Fig. 4) can again be understood by considering the role of tip-induced atomic displacements. In the absence of the tip, Cl^- ions over vacancies displace strongly outwards from the surface [0.04 nm; see Fig. 1(c)], while those over Cd^{2+} remain close to the ideal surface plane. This results in the strong difference in contrast over neighboring Cl^- ions seen at long range and is strongly enhanced due to large tip-induced displacements [see Fig. 3(d)]. The change in the profiles shown in Fig. 4(b) is due to two components: the reduction in repulsion over Na^+ ions due to displacements of neighboring Cl^- ions towards the tip at close approach [see Fig. 3(e)] and the increased attraction to the rigidly held Cl^- ion over a Cd^{2+} ion. The increase in the contribution of the Cl^- over Na^+ ion as the tip approaches the surface, as shown in Fig. 4(c), is also due to the displacement of the Cl^- ion towards the tip [see Fig. 3(f)]. The quantitative agreement between experiment and simulations highlights the ability of SFM to resolve the influence of impurities and defects, even subsurface, through its sensitivity to atomic displacements.

Our results show that all ions in the Suzuki structure can be identified by dynamic SFM imaging, thereby characterizing the tip's potential. This identification is possible due to the doping of NaCl with divalent impurity ions and thanks to the geometry of the atomic Suzuki structure, which contrasts the situation on pure NaCl [11]. It is shown that this can be done independently of the tip-surface distance, of the chemical nature of the divalent impurity ions, and despite differences in surface termination. Simulations show that the development of contrast patterns as a function of tip-surface separation on both surfaces is strongly linked to tip-induced atomic displacements, which is significantly different to the contrast formation on other cubic ionic surfaces.

The ready access to interpretation of atomically resolved images makes Suzuki surfaces an attractive choice for investigations of deposited molecules and nanoparticles. The chemical identification makes it much easier to characterize deposited nano-objects and reaction products at the atomic scale. An additional benefit is the ability to nanotemplate the surface with Suzuki regions of different electronic and reactive character. Several other Suzuki systems in NaCl exist, including the magnetic impurities Mn^{2+} and Fe^{2+} [25], which our calculations predict would form an antiferromagnetic ordering particularly suited to exchange force microscopy [26]. Other types of host system for the Suzuki phases such as oxides (MgO:Mn^{4+} [15]

and NiO:Mn^{4+} [27]) might also be interesting in nanocatalysis. We believe that doping of insulators, in combination with high resolution dynamic SFM, provides a general tool for characterizing surfaces at the atomic scale. The wide use of doping with impurities of different valences in many insulators such as ZrO_2 and CeO_2 [28,29] suggests that the method could also be used in high resolution studies of their surfaces [30].

[1] L. Nony *et al.*, Nano Lett. **4**, 2185 (2004).
[2] P. Liljeroth *et al.*, Science **317**, 1203 (2007).
[3] M. Fendrich and T. Kunstmann, Appl. Phys. Lett. **91**, 023101 (2007).
[4] T. Dienel *et al.*, Adv. Mater. **20**, 959 (2008).
[5] T. Glatzel *et al.*, Appl. Phys. Lett. **94**, 063303 (2009).
[6] Z. Gai *et al.*, Appl. Phys. Lett. **86**, 023107 (2005).
[7] C. Barth and C. R. Henry, Appl. Phys. Lett. **89**, 252119 (2006).
[8] M. Goryl *et al.*, Phys. Rev. B **76**, 075423 (2007).
[9] *Noncontact Atomic Force Microscopy*, edited by S. Morita, R. Wiesendanger, and E. Meyer (Springer, Berlin, 2002).
[10] W. Hofer *et al.*, Rev. Mod. Phys. **75**, 1287 (2003).
[11] R. Bennewitz *et al.*, Phys. Rev. B **62**, 2074 (2000).
[12] C. Barth and C. R. Henry, Phys. Rev. Lett. **91**, 196102 (2003).
[13] R. Hoffmann *et al.*, Phys. Rev. Lett. **92**, 146103 (2004).
[14] Y. Sugimoto *et al.*, Nature (London) **446**, 64 (2007).
[15] J. S. Kasper and J. S. Prenner, Acta Crystallogr. **7**, 246 (1954).
[16] K. Suzuki, J. Phys. Soc. Jpn. **16**, 67 (1961).
[17] C. Barth and C. R. Henry, Phys. Rev. Lett. **100**, 096101 (2008).
[18] G. Grange, Surf. Sci. **105**, 265 (1981).
[19] A. L. Shluger *et al.*, J. Phys. Condens. Matter **6**, 1825 (1994).
[20] R. W. Grimes *et al.*, J. Phys. Condens. Matter **1**, 7367 (1989).
[21] G. Kresse and J. Furthmüller, Phys. Rev. B **54**, 11 169 (1996).
[22] C. J. J. van Loon and D. J. W. Ijdo, Acta Crystallogr. Sect. B **31**, 770 (1975).
[23] M. Chall *et al.*, J. Phys. Chem. B **104**, 1191 (2000).
[24] See EPAPS Document No. E-PRLTAO-103-007929 for a detailed comparison between experimental and theoretical dynamic scanning force microscopy simulations of the Suzuki structure on (001) surfaces of Mg^{2+} or Cd^{2+} doped NaCl crystals presented as a reference library. For more information on EPAPS, see http://www.aip.org/pubservs/epaps.html.
[25] M. J. Yacamán and J. P. Hirth, Thin Solid Films **38**, 215 (1976).
[26] U. Kaiser *et al.*, Nature (London) **446**, 522 (2007).
[27] P. Porta *et al.*, J. Solid State Chem. **92**, 202 (1991).
[28] *Catalysis by Ceria and Related Materials*, edited by A. Trovarelli (Imperial College Press, London, 2006), Vol. 2.
[29] D. R. Ou *et al.*, Phys. Rev. B **77**, 024108 (2008).
[30] K. I. Fukui *et al.*, Appl. Surf. Sci. **188**, 252 (2002).